

Exposure of the Hybrid Detector of The Pierre Auger Observatory

Francesco Salamida*† for the Pierre Auger Collaboration

*University of L'Aquila & INFN, via Vetoio I, 67100, Coppito(AQ)

†Observatorio Pierre Auger, Av. San Martín Norte 304, Malargüe, (5613) Mendoza, Argentina

Abstract. The exposure of the Pierre Auger Observatory for events observed by the fluorescence detector in coincidence with at least one station of the surface detector is calculated. All relevant monitoring data collected during the operation, like the status of the detector, background light and atmospheric conditions are considered in both simulation and reconstruction. This allows to realistically reproduce time dependent data taking conditions and efficiencies.

I. INTRODUCTION

The measurement of the cosmic ray flux above 10^{18} eV is one of the foremost goals of the Pierre Auger Observatory [1]. In this energy region two different features, the *ankle* and the *GZK cut-off* are expected. In particular the transition between the galactic and the extragalactic component of cosmic rays [2] is widely believed to be associated with a flattening of cosmic rays energy spectrum, identified as the ankle. An accurate determination of the ankle could help to discriminate among theoretical models [3], [4], [5] describing this transition.

The hybrid approach is based on the detection of showers observed by the Fluorescence Detector (FD) in coincidence with at least one station of the Surface Detector (SD). Although a signal in a single station doesn't ensure an independent trigger and reconstruction in SD [6], it is a sufficient condition for a very accurate determination of the shower geometry using the hybrid reconstruction.

The measurement of cosmic ray flux relies on the precise determination of detector exposure that is influenced by several factors. The response of the hybrid detector is in fact very much dependent on energy, distance of recorded event, atmospheric and data taking conditions.

II. HYBRID EXPOSURE

The flux of cosmic rays J as a function of energy is defined as:

$$J(E) = \frac{d^4N}{dE dS d\Omega dt} \simeq \frac{1}{\Delta E} \frac{N^D(E)}{\mathcal{E}(E)}; \quad (1)$$

where $N^D(E)$ is the number of detected events in the energy bin centered around E having width ΔE on a surface element dS , solid angle $d\Omega$ and time dt , $\mathcal{E}(E)$ represents the energy dependent exposure of the detector.

The exposure, as a function of primary shower energy, can be written as:

$$\mathcal{E}(E) = \int_T \int_{\Omega} \int_{A_{gen}} \varepsilon(E, t, \theta, \phi) dS \cos \theta d\Omega dt; \quad (2)$$

where ε is the detection efficiency including analysis selection cuts, dS and A_{gen} are the differential and total Monte Carlo generation areas, respectively. The generation area A_{gen} has been chosen large enough to include the detector array with a sizable trigger efficiency. $d\Omega = \sin \theta d\theta d\phi$ and Ω are respectively the differential and total solid angles, being θ and ϕ the zenith and azimuth angles. The growth of surface array and ongoing extensions of the fluorescence detector, seasonal and instrumental effects obviously introduce changes of the detector configuration with time. All these effects can be taken into account by simulating a sample of events that reproduces the exact data taking conditions.

III. HYBRID ON-TIME

The calculation of hybrid exposure requires the knowledge of the detector on-time. The efficiency of fluorescence and hybrid data taking is influenced by many effects. These can be external, e.g. lightnings and storms, or internal, due to data taking inefficiencies, e.g. DAQ failures. To determine the on-time of our hybrid detector it is therefore crucial to take as many of these possibilities into account and derive a solid description of the time dependent data taking.

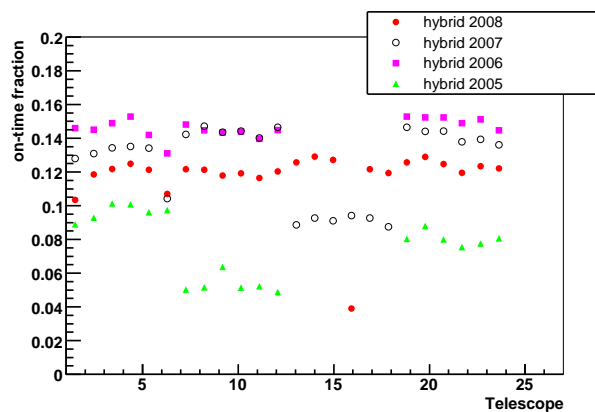


Fig. 1. The evolution of the average hybrid duty-cycle during the construction phase of the Pierre Auger Observatory.

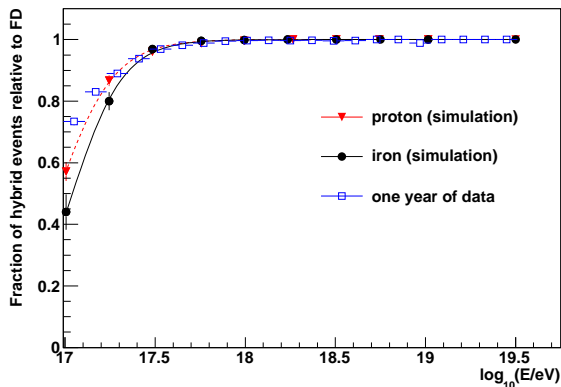


Fig. 2. Relative hybrid trigger efficiency from hybrid simulation for proton, iron and data. All the events are taken for zenith less than 60° .

Failures can occur on different levels starting from the smallest unit of the FD, i.e. one single PMT readout channel, up to the highest level, i.e. the combined SD-FD data taking of the Observatory.

The on-time of the hybrid detector has been derived using data and a variety of monitoring information. As compromise between accuracy and stability we derived the complete detector status down to the single photomultiplier for time intervals of 10 min.

The time evolution of the full hybrid duty-cycle over 4 years during the construction phase of the observatory is given in figure 1. It has to be noted that the telescopes belonging to the building of Los Morados (telescopes 7-12) have become operational only in May 2005 and the ones in Loma Amarilla (telescopes 13-18) in March 2007. Moreover the quality of the data taking increases from 2005 to 2007. The decrease of the average on-time in 2008 is due to the lowering of the maximum background value allowed for the FD data taking. The result has been cross-checked with other independent analyses [7], [8] giving an overall agreement within about 4%.

IV. MONTE CARLO SIMULATION AND EVENT SELECTION

To reproduce the exact working conditions of the experiment and the entire sequence of the different occurring configurations, a large sample of Monte Carlo events has been produced. The simulated data sample consists of longitudinal energy deposit profiles generated with the CONEX [12] code using QGSJet-II [10] and Sibyll 2.1 [11] as hadronic interaction models. As the distribution of particles at ground is not provided by CONEX, the time of the station with the highest signal is simulated according to the muon arrival time distribution [13]. This time is needed in the hybrid reconstruction for determining the incoming direction of the showers and the impact point at ground.

In order to validate such approach, a full hybrid simulation was performed using CORSIKA showers [15], in which FD and SD response are simultaneously and

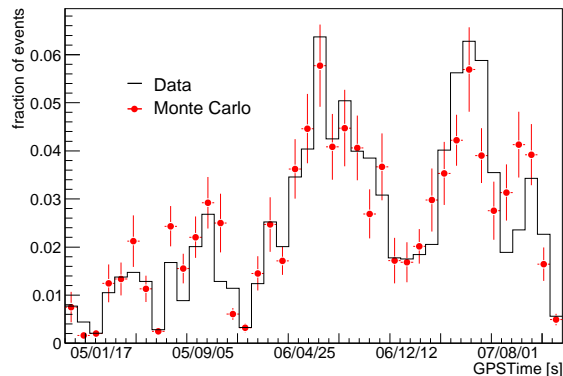


Fig. 3. Data-Monte Carlo Comparison: fraction of hybrid events as a function of time starting from November 2005. Both data (solid line) and simulations (solid circles) are shown.

fully simulated. As it is shown in Figure 2, the hybrid trigger efficiency (an FD event in coincidence with at least one SD station) is flat and equal to 1 at energies greater than 10^{18} eV. The difference between the two primaries becomes negligible for energies larger than $10^{17.5}$ eV. Furthermore the comparison with data shows a satisfactory agreement. The CORSIKA simulations have been also used to parameterize the response of the SD stations using the *Lateral Trigger Probability* functions [16].

The effect of the different data taking configurations has been taken into account and simulated using the calculation of the hybrid detector on-time. Moreover the impact of cloud coverage and atmospheric conditions on the exposure calculation has been taken into account using the information of the atmospheric monitoring [9] of the Pierre Auger Observatory. All the simulations were performed within the Auger analysis framework [14].

Once the shower geometry is known, the longitudinal profile can be reconstructed and the energy calculated

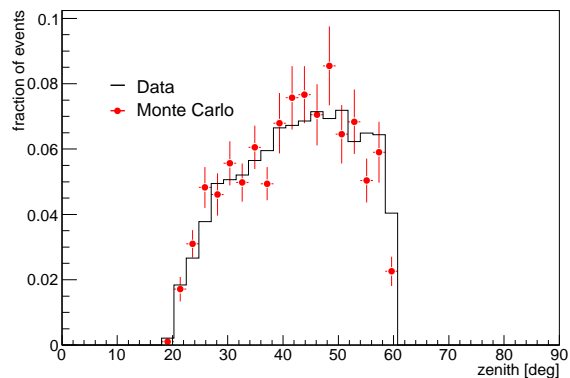


Fig. 4. Data-Monte Carlo Comparison: fraction of hybrid events as a function of the measured zenith angle for the events passing the quality cuts. Both data (solid line) and simulations (solid circles) are shown.

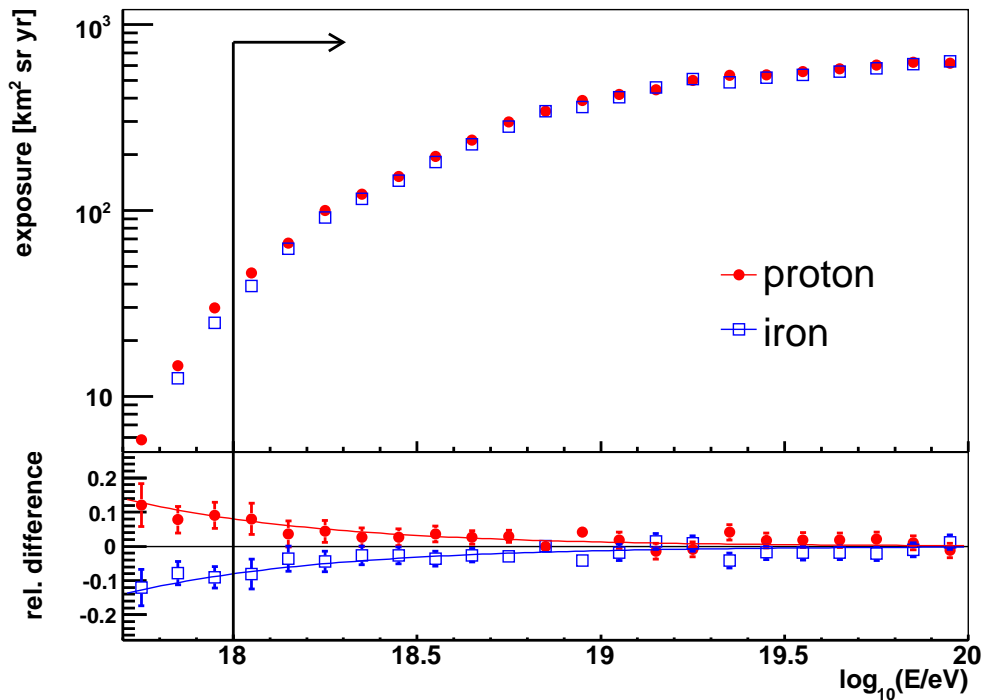


Fig. 5. The hybrid exposure for proton (solid dot) and iron (open squares) primaries derived from Monte Carlo simulation. The relative difference between pure proton(iron) exposure and a mixed composition exposure is shown in the lower panel.

in the same way as for data. The following quality cuts have been designed and used also for the hybrid spectrum.

A first set is based on the quality of the geometrical reconstruction:

- reconstructed zenith angle less than 60° ;
- station used for the hybrid reconstruction lying within 1500 m from the shower axis;
- energy dependent core-FD site distance according to [17];
- energy dependent field of view according to [18].

A second set of cuts is based on the quality of the reconstructed profile:

- a successful Gaisser-Hillas fit with $\chi^2/N_{dof} < 2.5$ for the reconstructed longitudinal profile.
- minimum observed depth $<$ depth at shower maximum (X_{max}) $<$ maximum observed depth;
- events with relative amount of Cherenkov light in the signal less than 50%;
- energy reconstruction uncertainty less than 20%;

A final set of cuts is based on the quality of the atmospheric conditions:

- measurement of atmospheric parameters available [19], [9];
- cloud coverage from Lidar measurements [9] lower than 25%.

The reliability of quality cuts has been checked by comparing the distributions of data and Monte Carlo for all the relevant shower observables. The fraction of selected hybrids events is shown in Figure 3 as a

function of time. In this plot both the growing of the hybrid detector and the seasonal trend of the hybrid data taking efficiency are visible. As an example the distributions of the measured zenith angle for both data and Monte Carlo are shown in Figure 4. In this plot only the events passing the quality cuts are shown. Data are in an agreement with simulations.

V. RESULTS

The hybrid exposure is shown in Figure 5 both for proton (solid dot) and iron (open squares) primaries. The black arrow indicates the region above 10^{18} eV where the exposure is used for the measurement of the hybrid spectrum. The exposure has been corrected for a 4% systematic inefficiency derived from the analysis of Central Laser Facility [19] shots. The residual difference between pure proton/iron exposure and a mixed composition (50% proton - 50% iron) one is about 8% at 10^{18} eV and decreases down to 1% at higher energies. The dependence of the exposure on the hadronic interaction model has been studied in detail by comparing the exposures obtained respectively with QGSJet-II and Sibyll 2.1 Monte Carlo events. The result shows that this effect is negligible.

The design of the Pierre Auger Observatory with its two complementary air shower detection techniques offers the chance to validate the full Monte Carlo simulation chain and the derived hybrid exposure with air shower observations themselves. Based on this end-to-end comparison the hybrid event rate from data has shown a discrepancy of 8% with respect to Monte Carlo

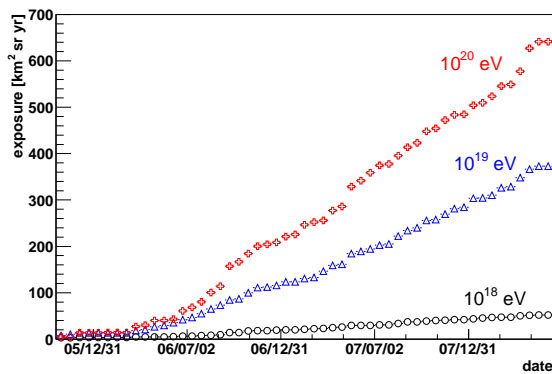


Fig. 6. The growth of the hybrid exposure as a function of time starting from November 2005 up to May 2008 for three different energies.

simulations. The exposure has been corrected for half of the observed difference and an upper limit of the systematic uncertainty of about 5% is estimated. Taking into account all these contributions the overall systematic uncertainty on the knowledge of the exposure ranges from 10% at 10^{18} eV to 6% above 10^{19} eV.

In Figure 6, the growth of the hybrid exposure as a function of time is shown for three different energies. The increase shown at each energy is not only related to the accumulation of data taking with time. In particular one can easily observe faster changes corresponding to the longer periods in the austral winter. The trend is also affected by the growth of the SD array in the corresponding period. This effect is more marked at higher energies where a bigger hybrid detection volume is accessible with new SD stations.

VI. CONCLUSIONS

A time dependent Monte Carlo simulation has been performed and the exposure of the hybrid detector of the Pierre Auger Observatory has been derived. The use of the monitoring information of the Pierre Auger Observatory allows to follow in detail the changes in the data taking configuration and atmospheric conditions as confirmed by the comparison between data and Monte Carlo. This procedure ensures a systematic uncertainty on the knowledge of the exposure lower than 10% on the entire energy range used for the measurement of the hybrid spectrum [1].

REFERENCES

- [1] F. Schüssler for the Pierre Auger Collaboration, *Proc. 31th Int. Cosmic Ray Conf. (Lodz, Poland)*, 2009.
- [2] J. Linsley, *Proc. 8th Int. Cosmic Ray Conf. (Jaipur)*, 77-99, 1963.
- [3] V.S. Berezinsky, A.Z. Gazizov and S.I. Grigorieva, *Phys. Rev.*, D74, p. 043005, 2006.
- [4] D. Allard, E. Parizot and A. Olinto, *Astrop. Phys.*, 27, 61-75, 2007.
- [5] J.N. Bahcall and E. Waxman, *Phys. Lett.*, B556, 1-6, 2003.
- [6] J. Abraham et al. [Pierre Auger Collab.], *Phys. Rev. Letters*, 101, p. 061101, 2008.

- [7] The Fluorescence Detector of the Pierre Auger Observatory, paper in preparation.
- [8] J. Rautenberg for the Pierre Auger Collaboration, *Proc. 31th Int. Cosmic Ray Conf. (Lodz, Poland)*, 2009.
- [9] S.Y. BenZvi for the Pierre Auger Collaboration, *Proc. 31th Int. Cosmic Ray Conf. (Lodz, Poland)*, 2009.
- [10] S. Ostapchenko, *Nucl. Phys. B(Proc. Suppl.)*, 151:143, 2006.
- [11] R. Engel et al., *Proc. 26th Int. Cosmic Ray Conf. (Salt Lake City, USA)*, 415, 1999.
- [12] T. Bergmann et al, *Astropart. Phys.* 26, 420, 2007.
- [13] L. Cazón et al., *Astrop. Phys* 21, 71-86, 2004.
- [14] L. Prado et al, *Nucl. Instr. Meth.* A545, 632, 2005.
- [15] D. Heck et al, *Report FZKA 6019*, 1998.
- [16] E. Parizot for the Pierre Auger Collaboration, *Proc. 29th Int. Cosmic Ray Conf. (Pune, India)*, 7, 71-74, 2005.
- [17] J. Abraham et al. [Pierre Auger Collab.], *Astropart. Phys.* 27, 2007.
- [18] M. Unger for the Pierre Auger Collaboration, *Proc. 30th Int. Cosmic Ray Conf. (Merida, Mexico)*, arXiv:0706.1495, 2007.
- [19] L. Valore for the Pierre Auger Collaboration, *Proc. 31th Int. Cosmic Ray Conf. (Lodz, Poland)*, 2009.